Interannual Variability of Sea Surface Temperature in the Southwest Pacific and the Role of Ocean Dynamics

MELISSA BOWEN AND JORDAN MARKHAM

School of Environment, University of Auckland, Auckland, New Zealand

PHILIP SUTTON

National Institute of Water and Atmospheric Research, Wellington, New Zealand

XUEBIN ZHANG AND QURAN WU

CSIRO Oceans and Atmospheres, Hobart, Australia

NICK T. SHEARS

Leigh Marine Laboratory, Institute of Marine Science, University of Auckland, Auckland, New Zealand

DENISE FERNANDEZ

National Institute of Water and Atmospheric Research, Wellington, New Zealand

(Manuscript received 29 November 2016, in final form 2 June 2017)

ABSTRACT

This paper investigates the mechanisms causing interannual variability of upper ocean heat content and sea surface temperature (SST) in the southwest Pacific. Using the ECCOv4 ocean reanalysis it is shown that air–sea heat flux and ocean heat transport convergence due to ocean dynamics both contribute to the variability of upper ocean temperatures around New Zealand. The ocean dynamics responsible for the ocean heat transport convergence are investigated. It is shown that SSTs are significantly correlated with the arrival of barotropic Rossby waves estimated from the South Pacific wind stress over the latitudes of New Zealand. Both Argo observations and the ECCOv4 reanalysis show deep isotherms fluctuate coherently around the country. The authors suggest that the depth of the thermocline around New Zealand adjusts to changes in the South Pacific winds, modifies the vertical advection of heat into the upper ocean, and contributes to the interannual variability of SST in the region.

1. Introduction

Sea surface temperature (SST) plays a central role in weather and climate due to its influence on the transfer of heat and moisture between the ocean and the atmosphere. Determining what causes SST to vary is challenging because it is the result of many processes in both the atmosphere and the ocean [see Deser et al. (2010) for a review]. In the midlatitudes of the Southern Hemisphere, SST is often significantly correlated with El Niño–Southern Oscillation (ENSO) (Greig et al. 1988; Holbrook and Bindoff 1997; Fauchereau et al. 2003), suggesting a connection to large-scale changes in the atmosphere in response to changes at the equatorial Pacific.

It is unclear what processes may be causing the correlation between SST and ENSO in the southwest Pacific. Several studies have investigated the communication of an ENSO signal by the atmosphere during summer when mixed layer depths are shallow and SST is more likely to reflect changes in air–sea exchange. Fauchereau et al. (2003) find that summer SST anomalies in the Tasman Sea are correlated with ENSO and are also correlated with SST in the South Atlantic and Indian Oceans. They suggest that the variations are caused by changes in the

Corresponding author: Melissa Bowen, m.bowen@auckland.ac.nz

DOI: 10.1175/JCLI-D-16-0852.1

latent heat flux due to changes in the wind speed. Ciasto and England (2011) examine the upper-ocean heat balance in summer months from reanalysis products and show that SST anomalies in the southwest Pacific are not well described by air–sea heat exchange or advection of heat by Ekman transport. Their results suggest that other terms in the heat balance cannot be neglected, such as the horizontal transport of heat by ocean currents and the vertical movement of heat by advection and entrainment. Guan et al. (2014) find that variations in latent heat flux driven by the winds are largely responsible for large-scale variation of SST anomalies over the South Pacific; however, they suggest that local Ekman pumping may play a role in SST anomalies around New Zealand.

Changes in SST have also been linked to the horizontal transport of heat by ocean currents and to changes in midlatitude winds. Wu et al. (2012) link increasing SSTs in all three Southern Hemisphere subtropical western boundary currents, including the East Australian Current, to changes in wind stress curl over the ocean basins increasing transport or shifting the boundary currents. Hill et al. (2008) explain the trends and variations in temperature at Maria Island, Tasmania, as the result of changes in transport in the East Australian Current Extension in response to South Pacific winds. In the Subantarctic Front south of Tasmania, Rintoul and England (2002) find that meridional Ekman transport is instrumental in creating temperature anomalies. Ummenhofer and England (2007) find marked changes in the Ekman transport between different phases of the southern annular mode (SAM) and Southern Oscillation index (SOI) over the southwest Pacific, but they question whether the heat advection by the Ekman transport is of a sufficient magnitude to play a leading role and whether it has the correct phase to drive SST variations.

The relationship between SST and temperatures below the mixed layer has been investigated in several studies using the expendable bathythermograph (XBT) lines around New Zealand. Ciasto and Thompson (2009) estimate that about 20% of the interannual variability of SST in the southwest Pacific can be related to the ''reemergence'' of temperature anomalies from the previous winter mixed layer. Sprintall et al. (1995) use temperatures on the PX06, PX34, and PX30 XBT lines between Australia, New Zealand, and New Caledonia to show that a divergence of geostrophic velocities in the upper 800 m in the Tasman Sea occurred at the same time as anomalously cold SSTs and air temperatures in New Zealand in the early 1990s. They suggest that the exit of warm water from the region leaves cooler water beneath the mixed layer and ''preconditions'' the upper ocean to cooler temperatures. Sutton et al. (2005) show that temperatures from the surface to 800 m along the PX34 XBT line across the Tasman Sea vary together through the 1990s and early 2000s. They suggest that temperatures at all depths are responding to the same mechanism and note that local Ekman pumping is not able to explain the movement of the isotherms.

A number of studies have described the adjustment of subsurface temperatures and sea level in the region. Bowen et al. (2006) show the movement of the isotherms at depth along the XBT line north of New Zealand can largely be explained by wind-forced baroclinic Rossby waves. Sasaki et al. (2008) show that the propagation of coastal waves around New Zealand, excited by baroclinic Rossby waves arriving along the east coast, explains much of sea level variation in the Tasman Sea on the western side of New Zealand. They show that SST and sea surface height (SSH) vary together over a wide region of the South Pacific and suggest the correspondence may be due to Ekman pumping and wave propagation. Hill et al. (2011) investigate the adjustment of the South Pacific in a series of ocean general circulation model simulations. Their simulations show that barotropic Rossby waves, created by a change in wind stress over the South Pacific, propagate quickly across the Pacific to the eastern New Zealand coast and generate baroclinic coastal waves that propagate anticlockwise around New Zealand. On the western side of the country, baroclinic Rossby waves radiate from the coast and propagate across the Tasman Sea to Australia. These studies suggest that the thermocline around New Zealand responds coherently to changes in the wind stress curl across the South Pacific.

In summary, previous studies vary widely on what may be causing interannual variations of SST in the southwest Pacific. However, the correspondence between surface and subsurface ocean temperature suggests that heat exchange between the upper ocean and the deeper ocean deserves further investigation. In this study, we investigate the role of ocean dynamics in the upper-ocean heat balance, making use of long time series of surface ocean observations at the Leigh Marine Station in northern New Zealand and the subsurface temperature records along the XBT lines around the country (Fig. 1). We first examine the interannual variability in sea surface temperature from the 49-yr record at Leigh. We show that this coastal temperature record is representative of a much wider area of the southwest Pacific. We compare the temperature record to estimates of air–sea heat flux and the arrival of Rossby waves at the New Zealand coast. We then examine the heat balance from observations and an ocean reanalysis. Finally, we discuss the contributions of different mechanisms to the interannual variability of sea surface temperature around New Zealand.

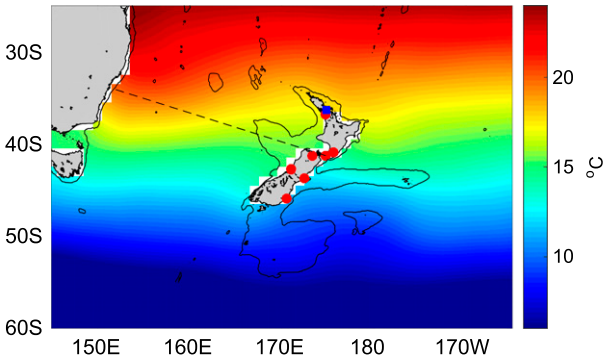

FIG. 1. The southwest Pacific with the location of the Leigh Marine Station (blue) and the NZ T7 air temperature stations (red). Background colors show the mean SST from the satellite record and the 1000-m isobath is shown in black. The black dashed line shows the location of the PX34 XBT line between Wellington and Sydney.

2. Methods

a. Observations

1) OCEAN AND AIR TEMPERATURES

Interannual variations of sea surface temperature in the southwest Pacific are examined using two different time series. The first is a record spanning the last 49 years collected at the Leigh Marine Laboratory in northern New Zealand (Fig. 1). From 1967 to 2009, surface sea temperatures were measured at 9 a.m. daily using a bucket and a calibrated mercury thermometer (Evans and Atkins 2008). Short gaps in this record comprise only 123 missing days in total or 0.8% of the total time. Since 2011, surface temperatures have been measured from a moored thermistor located 100 m from the original collection site. Monthly means were created from these time series using the bucket data and the 9 a.m. temperature reading from the moored thermistor. Two gaps in the time series, May–September 2011 and March–June 2013, were estimated using the relationship between the regression of the monthly values with monthly values at Leigh from the NOAA OISST product (Reynolds et al. 2002) at the nearest grid point 600 m to the west.

Sea surface temperatures from the NOAA OISST product were also used to look at variability in sea surface temperatures over the southwest Pacific from November 1981 to April 2016. SST anomalies were created by subtracting the monthly means over the entire record from each monthly value. The monthly anomalies were then low-pass filtered using a cosine window with a half-period of 13 months. Annually averaged anomalies were created from all the other datasets in an identical manner.

Two datasets were used to investigate subsurface ocean temperatures. Temperatures over the upper 2000 m were investigated using an optimal interpolation of Argo data, the Roemmich and Gilson climatology (Roemmich and Gilson 2009). The Argo product uses the nearest 100 Argo profiles to estimate monthly temperature and salinity with depth at each degree of latitude and longitude from 2004 to present. Ocean temperatures from the World Ocean Circulation Experiment (WOCE) repeat high-resolution PX34 line between Wellington and Sydney were used to examine temperature changes in the upper 800 m of the Tasman Sea (Fig. 1). The transect is sampled about four times a year with XBTs deployed from container ships.

New Zealand air temperatures were compared with sea surface temperatures using the New Zealand seven-station temperature anomaly (NZT7). The NZT7 is calculated by subtracting the 1981–2010 temperature averaged over the seven stations (Auckland, Masterton, Wellington, Nelson, Hokitika, Lincoln, and Dunedin; Fig. 1) from the monthly average of the seven stations (Folland and Salinger 1995; Mullan et al. 2010). The monthly anomalies were low-pass filtered to compare with the ocean temperatures.

2) CLIMATE INDICES AND SEA SURFACE HEIGHT

Interannual variations in the sea surface and air temperature records were compared to changes in the equatorial Pacific by correlating with the Southern Oscillation index. Monthly values of the SOI, calculated from the difference in atmospheric pressure between Tahiti and Darwin, were obtained from the Australian Bureau of Meteorology and divided by 10.

SSH anomalies were used to investigate the adjustment of sea level around New Zealand. The mapped sea level anomalies (MSLAs) were obtained from AVISO (Ducet and LeTraon 2000) and use all available altimeter observations from October 1992 to April 2016. Aliasing of the M2 tide was removed from the anomalies by averaging over the alias period. Absolute surface geostrophic velocities from the same time period were also obtained from AVISO to estimate the contribution of geostrophic ocean flow to the upper-ocean heat balance.

3) ATMOSPHERIC AND OCEANIC REANALYSIS PRODUCTS

The transfer of heat and momentum between the atmosphere and ocean was estimated using the Japanese 55-Year Reanalysis (JRA-55) fluxes (Kobayashi et al. 2015). The net radiative and turbulent heat fluxes were compared to the change in temperature at Leigh. The JRA-55 momentum fluxes are used to estimate changes

in the South Pacific wind stress and Ekman pumping. Heat fluxes from the OAFlux project (Yu and Weller 2007), which combines satellite and surface meteorology to better estimate surface fluxes, are also compared to the other heat fluxes at Leigh and the temperature change at Leigh.

The terms in the heat balance from the Estimating the Circulation and Climate of the Ocean (ECCO) ocean state estimate version 4 (Forget et al. 2015) were used to diagnose the upper ocean heat budget in the Tasman Sea between 1992 and 2011. The ECCOv4 solution brings the atmospheric reanalyses and ocean observations into consistency with the model equations [from the Massachusetts Institute of Technology GCM (MITgcm)] by adjusting the initial ocean conditions, atmospheric forcing, and subgrid parameters iteratively. The resulting model outputs are consistent with the ocean observations within a certain error, and all the heat and momentum budgets are closed. The initial atmospheric fluxes in the ECCOv4 reanalysis are the ERA-Interim reanalysis; the final fluxes have been adjusted to be more consistent with the ocean observations. The GECCO2 ocean state estimate (Köhl 2015) is similar to the ECCOv4 reanalysis but extends back further in time (1948–2011) and uses the NCEP atmospheric reanalysis as the initial fluxes. There are fewer measurements constraining the ocean state estimate prior to the 1990s when the XBT lines and satellite altimeter measurements began. For that reason, we use the GECCO2 reanalysis only to compare with the temperatures at Leigh.

b. Analysis

1) The upper-ocean heat balance

We investigate the upper-ocean heat balance in two ways: we estimate the terms in the heat balance using observations and we also examine the terms in the heat balance from an ocean state estimate.

The heat balance at a point can be expressed as the sum of temperature tendency and advective and diffusive fluxes on the left side and sources and sinks of heat on the right side:

$$\rho c_p\left[\frac{\partial T}{\partial t}+\frac{\partial (uT)}{\partial x}+\frac{\partial (vT)}{\partial y}+\frac{\partial (wT)}{\partial z}-\frac{\partial}{\partial z}\left(k_z\frac{\partial T}{\partial z}\right)\right]=\frac{\partial q}{\partial z}, \tag{1}$$

where T is temperature, ρ and c_p are the density and heat capacity of the water, respectively, and q is a source of heat. The exchange of heat by turbulent fluctuations is expressed with a vertical diffusivity (k_z), and only the vertical turbulent diffusion terms have been retained.

Integrating from the surface down to a fixed depth h, gives a heat balance for the upper ocean:

$$\frac{\partial}{\partial t}\int_{-h}^{0}\rho c_p T\,dz=-\int_{-h}^{0}\rho c_p\left[\frac{\partial (uT)}{\partial x}+\frac{\partial (vT)}{\partial y}\right]dz+\rho c_p\left[wT+k_z\frac{\partial T}{\partial z}\right]\Bigg|_{-h}+Q. \tag{2}$$

The left side is the tendency of the upper-ocean heat content, which is due to the convergence of horizontal heat transport in the upper ocean (first term on the right side); the vertical advection and diffusion of heat (second term); and the sources and sinks of heat, Q, from interaction with the atmosphere. We use the air–sea heat flux at the surface and assume all the radiative fluxes are contained within the depth of the integration. Summed together, the horizontal and vertical advection of heat constitute the ocean heat transport convergence in the upper layer of depth h.

Ideally, we would like to integrate over an upper-layer depth that describes the interannual variation of ocean heat content available to the atmosphere. Previous studies use the maximum depth of the seasonal mixed layer (Roberts et al. 2017), and we use the same criteria for the heat balance from the ECCOv4 reanalysis. We integrate over the top 250 m, a depth that contains the entire mixed layer over the region. At 250 m, vertical diffusion is small and we can focus on the contribution of advection to the upper-ocean heat content.

We also examine the contributions of surface heat flux and convergence of heat transport individually to the upper-ocean temperature by integrating these terms separately with time, assuming constant values for c_p and ρ:

$$T_{\text{shf}}=\int\frac{Q}{\rho c_p h}dt, \tag{3}$$

$$T_{\text{conv}}=\int\left\{[wT]_{-h}-\int_{-h}^{0}\left[\frac{\partial (uT)}{\partial x}+\frac{\partial (vT)}{\partial y}\right]dz\right\}dt. \tag{4}$$

For the heat balance derived from observations, the only available temperature for the upper ocean is the sea surface temperature. For that reason, we integrate over the top 70 m, which is the average mixed layer depth from the Ifremer climatology (de Boyer Montgut et al. 2004), and use the sea surface temperature as representative of the temperature over that depth. This choice is consistent with other studies of the interannual upper-ocean heat balance from observations such as those of Verdy et al. (2006). We calculate the contribution of Ekman transport and geostrophic currents separately, using the geostrophic velocities and the Ekman transport from the wind stress: $u=u_{\text{Ek}}+u_{\text{Geo}}$.

For both the observations and the ECCOv4 analysis, the interannual anomaly of each term was created by subtracting the average monthly value of each term from the monthly values. The monthly anomalies were then low-pass filtered using a cosine filter with a half period of 13 months.

2) Barotropic Rossby wave model

The winds across the South Pacific are used to estimate the sea level changes due to the arrival of barotropic Rossby waves along the east coast of New Zealand. Barotropic Rossby waves travel quickly across the Pacific (in days to weeks) and a steady-state Sverdrup balance (Frankignoul et al. 1997) is used to derive sea level from monthly JRA-55 wind stress:

$$\eta = \frac{f^2}{\beta g H \rho_0} \int_{x_w}^{x_e} \nabla \times \frac{\tau}{f} dx, \tag{5}$$

where x_e and x_w are the locations of the eastern and western boundaries of the South Pacific respectively and H is the mean depth of the ocean basin, taken here as 4000 m. Integrating the sea level anomaly from the southern to northern extent of New Zealand (48°–35°S) and low-pass filtering gives an estimate of the sea level change due to the arrival of wind-driven barotropic Rossby waves. The time dependence of the sea level is proportional to the wind stress curl. It differs from the Island Rule transport (Godfrey 1989) only by the additional Ekman transport between New Zealand and South America. Neglecting the time-dependent term is appropriate for the rapid movement of barotropic Rossby waves and the adjustment of sea level and the thermocline by coastally trapped waves, which move around the country within a few months (Hill et al. 2011).

3) Correlations and significance

All correlations reported have been taken after removing trends from both time series. The significance of the correlations is reported using a p value associated with the correlation coefficient and the degrees of freedom. The degrees of freedom are found by dividing the length of the time series by an integral time scale, which was estimated from the autocovariance function of each time series by integrating to the first zero crossing and dividing by the value of the autocovariance at the origin (Emery and Thomson 2001).

3. Sea surface temperatures at Leigh

Temperatures at Leigh (Fig. 2) vary interannually with a standard deviation of 0.5°C. The variations in ocean temperatures are highly correlated with the New Zealand T7 air temperature anomalies ($r = 0.86; p < 0.001$). Both air and ocean temperatures are significantly correlated with the SOI ($r = 0.66; p < 0.001$ for sea and $r = 0.49; p < 0.001$ for air; Fig. 2), which suggests both are responding to large-scale changes in the atmosphere and ocean. The e-folding time scale of the SST autocorrelation function is 3.5 months, similar to e-folding time scales of midlatitude SST in other studies (Deser et al. 2003).

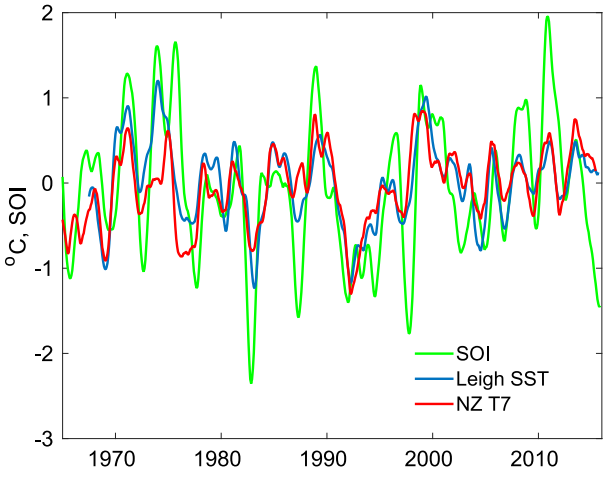

FIG. 2. Sea surface temperature at Leigh (blue), the Southern Oscillation index (green), and the NZ T7 air temperature (red). The temperature time series have had the seasonal cycle removed and are low-pass filtered.

Temperature anomalies at Leigh are highly correlated with ocean temperatures over a wide region around New Zealand. Annual anomalies at Leigh vary coherently with the annual anomalies of satellite sea surface temperatures over a large area of temperatures in the southwest Pacific (Fig. 3) and correlations of the monthly anomalies have similar magnitudes and patterns. The high correlations suggest SST at Leigh and a large area of ocean surrounding New Zealand are responding to the same large-scale processes in the atmosphere and ocean.

The high correlations between temperatures at Leigh, which is on the east coast of New Zealand, and the temperatures along the west coast of New Zealand suggest that coastal upwelling has little influence on the SST at Leigh. The same wind direction would cause the opposite response in coastal upwelling or downwelling on the east coast versus the west coast of New Zealand, which would lead to poorly or negatively correlated SST between the two coasts. Previous studies link SST variations along the NE New Zealand shelf to local Ekman transport (Sharples 1997), modulated by the ENSO variations in the alongshore wind stress (Zeldis et al.

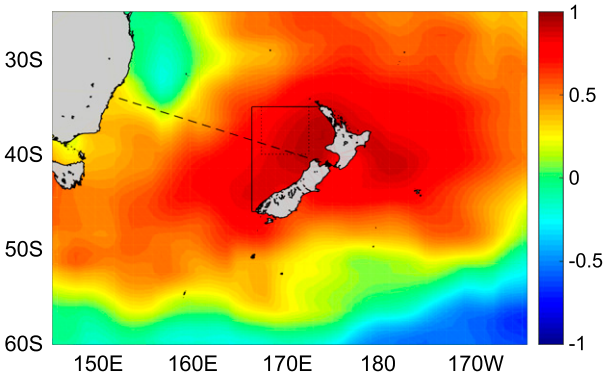

FIG. 3. The correlation of the Leigh temperatures with satellite SST over the period 1981 to 2015. The temperature time series have had the seasonal cycle removed and are smoothed annually before correlating. The box in the Tasman Sea is the region where the upper-ocean heat balance is examined in the ocean state analysis. The dotted lines show the region of the observational heat budget analysis. The black dashed line shows the PX34 XBT line.

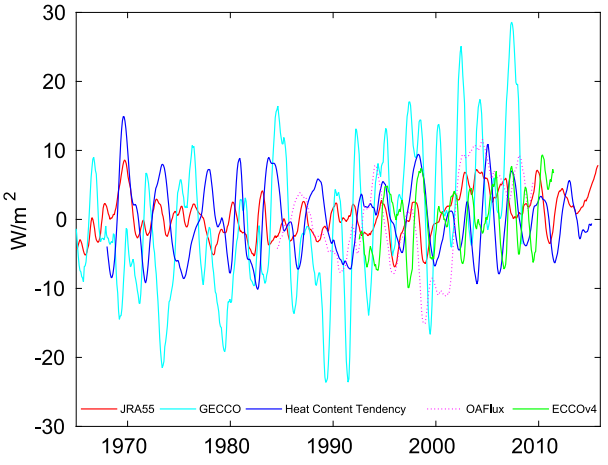

FIG. 4. Net surface heat flux over a 2° × 2° region around Leigh from the JRA-55 reanalysis (red), the GECCO2 ocean state estimate (light blue), the ECCOv4 ocean state estimate (green), and the OAFlux project (magenta) are compared to the upper-ocean heat content tendency estimated from the Leigh time series (blue). Positive heat flux is into the ocean.

2004). However, we also examined the daily temperature data and could find no correspondence between alongshore winds and temperature changes at Leigh, even at shorter times of a day to weeks.

One possible reason for the correlation of temperature over a wide geographic region around Leigh is that temperature may be largely driven by the exchange of heat between the atmosphere and ocean. To examine this at Leigh, Fig. 4 shows the interannual heat flux anomaly from the JRA-55 reanalysis, the ECCOv4 reanalysis, the GECCO reanalysis, and the OAFlux project, all averaged over two degrees of latitude and longitude around Leigh. The tendency of upper-ocean heat content at Leigh is found by taking the tendency of the low-pass filtered, seasonal anomaly temperatures (Fig. 4, blue line) and multiplying by $\rho c_p h$, where h is 70 m (the mean mixed layer depth in the northern New Zealand area). The tendency of upper-ocean heat content is not significantly correlated with any of the heat fluxes. There is considerable variation in the different heat flux products, suggesting large uncertainty in determining the actual value of air–sea heat flux.

The temperature at Leigh is also compared to the arrival of barotropic Rossby waves to examine potential connections between sea surface temperature and ocean adjustment around New Zealand (Fig. 5). The arrival of barotropic Rossby waves is highly correlated with the Leigh temperatures ($r = 0.64; p < 0.001$) and with the SOI ($r = 0.55; p < 0.001$). This correlation suggests there may be a connection between the arrival of barotropic waves and adjustment of the thermocline around the country. However, an examination of the heat balance is required to understand the role of each term in the interannual temperature variations at Leigh and the surrounding region (Fig. 3). Since Leigh is adjacent to the strong East Auckland Current, we investigate the heat balance in the eastern Tasman Sea where temperatures are highly correlated with those at Leigh.

4. The upper ocean heat balance in the eastern Tasman Sea

We first examine the upper ocean heat balance directly from observations in a 5° × 5° region in the eastern Tasman Sea (35°–40°S, 167°–172°E; see dotted box in Fig. 3). Terms in the heat budget of the upper 70 m from the observations show that temperature tendency and air–sea heat flux are usually the largest terms and correlated with each other (Fig. 6, upper panel). Advection of heat by Ekman and geostrophic currents are smaller. As noted by Ummenhofer and England (2007), the Ekman transport does not have the right phase to drive the temperature changes. Local vertical velocities from Ekman pumping, calculated from the wind stress curl, are not clearly related to changes in temperature (Fig. 6). Wind stress magnitude anomaly over the region is not highly correlated with temperature tendency (Fig. 6, lower panel), suggesting that wind-driven changes in vertical mixing or latent heat flux are not primarily responsible for the temperature changes. Thus, from the terms that can be calculated directly from observations, only the air–sea flux appears to be a likely dominant driver.

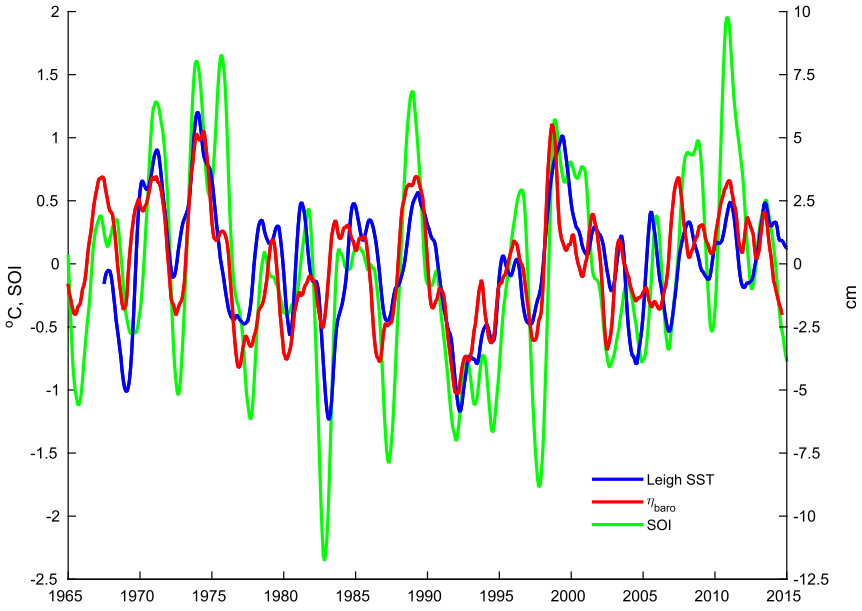

FIG. 5. Temperature anomaly at Leigh (blue) and sea level anomaly due to the arrival of barotropic Rossby waves (red) and the SOI (green).

The heat balance from the ECCOv4 ocean state estimate is closed, which allows an investigation of all of the terms in the heat balance, including the total contribution of ocean heat transport convergence. The heat budget over the entire eastern Tasman Sea (Fig. 3; solid box), where subsurface observations from the XBT line constrain the ocean state estimate, shows that advection by the horizontal and vertical velocities is the largest contribution to changes in heat content (Fig. 7, upper panel) and that the horizontal and vertical advection are anticorrelated with each other. The ocean heat transport convergence can be found by summing the terms and

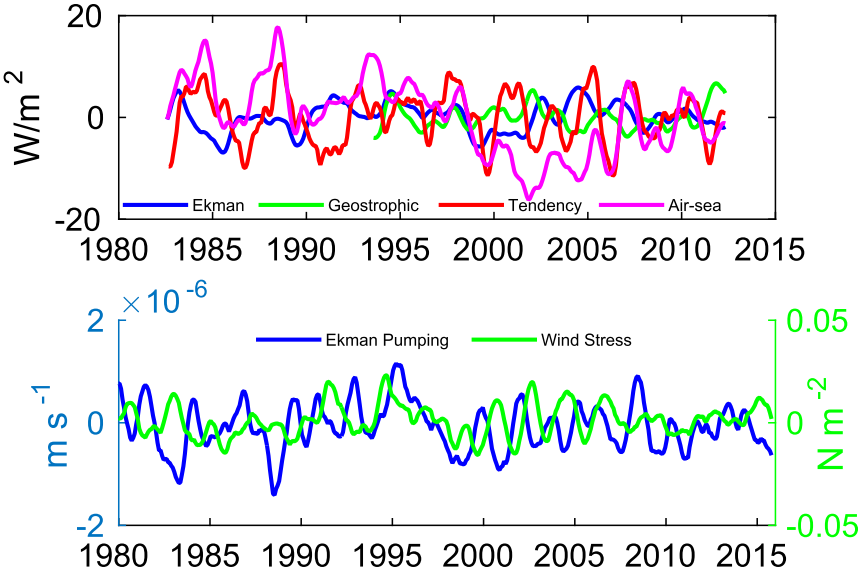

FIG. 6. (top) Temperature tendency (red), heat flux from the JRA-55 reanalysis (magenta), convergence of heat by Ekman transport (blue), and convergence of heat by geostrophic currents (green) estimated for the upper 70 m within 35°–40°S, 167°–172°E. (bottom) The Ekman pumping anomaly (blue) and anomaly of the wind stress magnitude (green) over the same area.

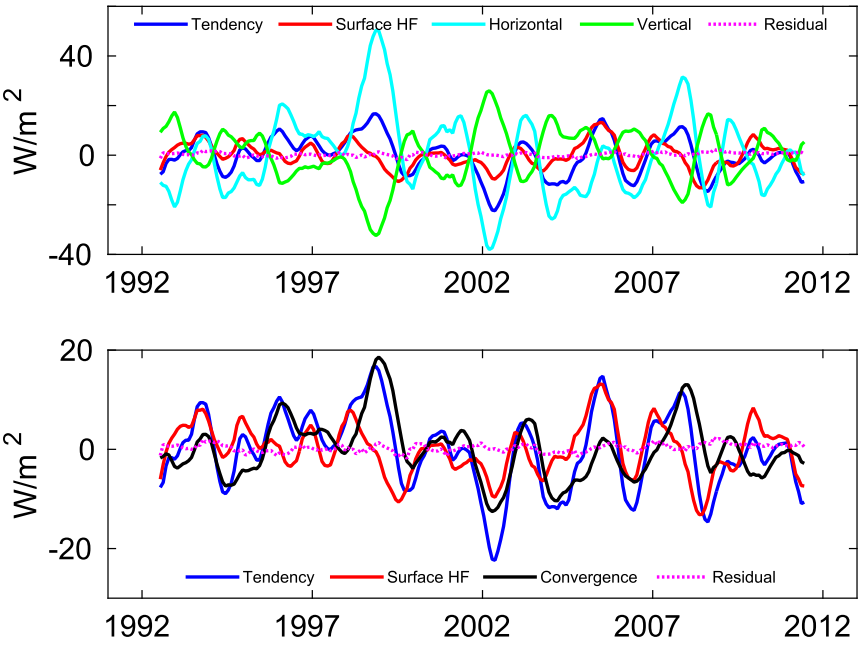

FIG. 7. (top) Terms from the ECCOv4 heat balance of the upper 250 m in the eastern Tasman Sea box: temperature tendency (blue), surface heat flux (red), horizontal convergence of heat (light blue), and vertical convergence of heat (green). The small residual term (magenta) contains the diffusion across the bottom boundary and the sides of the box. (bottom) As at top, but with the total ocean heat convergence, the sum of the vertical and horizontal terms, in black.

comparing with the surface heat flux and upper-ocean heat content tendency (Fig. 7, lower panel). The contribution of each term to the temperature anomaly is found by integrating each term as shown in Eqs. (4) and (5) (Fig. 8). The contribution to the temperature anomaly by ocean heat transport convergence is often larger than the surface heat flux: the standard deviation of the tendency, convergence, and surface heat flux terms are 8, 6, and 5 $\mathrm{W\,m^{-2}}$, respectively. The contribution of convergence is particularly evident from 1995 to 2002, when convergence is responsible for the warm anomalies that develop.

The vertical movement of isotherms at 250-m depth, a depth below the maximum winter mixed layer depth, illustrates the convergence and divergence of heat in the upper ocean. Temperatures along the Tasman XBT line (Fig. 9) increase in the late 1990s and drop between 2002 and 2005. Since 2005, there is less variability in temperature at 250 m in both the Argo observations and the XBT line. The ECCOv4 temperatures show similar variations. If the temperature changes in the XBT and Argo observations at 250 m are entirely due to vertical advection, then the resultant vertical velocities would have standard deviations of $4\times10^{-6}\,\mathrm{m\,s^{-1}}$ or $140\,\mathrm{m\,yr^{-1}}$, which are of a comparable magnitude to the vertical velocities in ECCOv4. Ekman transport across the boundaries of the box fluctuates between convergence and divergence of mass in the region, with Ekman pumping velocities of $\pm3\times10^{-7}\,\mathrm{m\,s^{-1}}$ or an order of magnitude lower than the vertical velocities estimated from the ocean observations, suggesting that local Ekman pumping is too weak to cause the movement of the isotherms.

To gauge the potential contribution of fluctuating vertical velocities to the upper-ocean heat budget over the South Pacific, the standard deviation of the vertical heat advection is plotted from the ECCOv4 ocean state estimate a depth 50 m below the maximum seasonal mixed layer depth at every location (Fig. 10). The vertical advection of heat is large in regions with more mesoscale activity (the East Australian Current, the confluence region south of Chatham Rise and the South Equatorial Current region), but also in regions of highly sloping bathymetry, such as the New Zealand continental shelf and the Kermadec Ridge. These regions are where vertical advection of heat can potentially contribute to the evolution of upper ocean temperatures.

5. Summary discussion

We have investigated the causes of interannual variability of sea surface temperature in the southwest

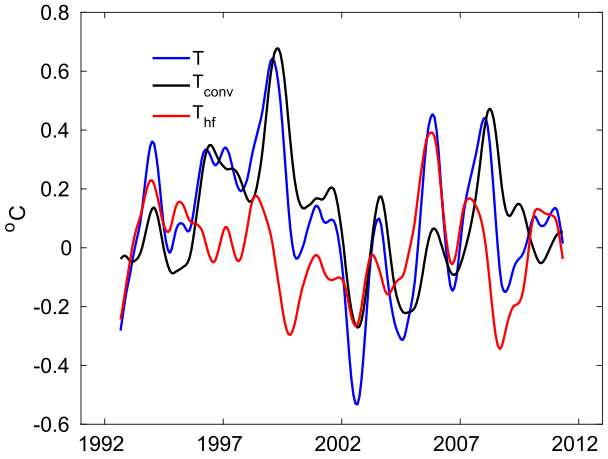

FIG. 8. The contribution of ocean heat transport convergence (black) and surface heat flux (red) to the total upper ocean temperature anomaly (blue).

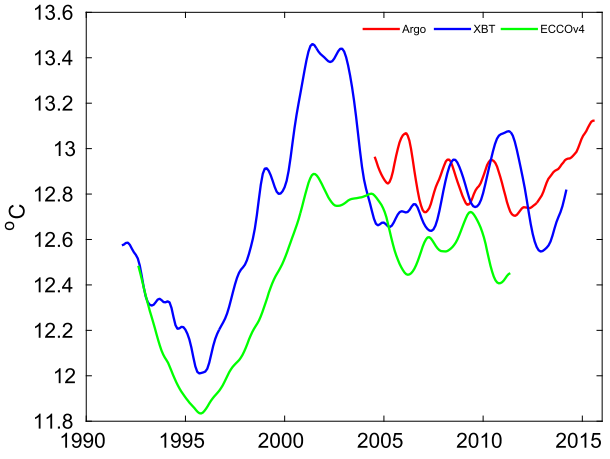

FIG. 9. Temperature at 250 m from the XBT line between 166°E and the New Zealand coast (blue) and from the RG Argo climatology (red) and ECCOv4 (green) averaged over a region around the XBT line.

Pacific and find no evidence for a single mechanism dominating the heat balance. Horizontal advection of heat alone does not explain the temperature variations. Neither Ekman nor geostrophic currents are the largest terms in the heat balance of the Tasman Sea (Fig. 7). Ummenhofer and England (2007) also noted that Ekman transport was too small in magnitude and of the wrong phase to explain interannual variations in temperature. The horizontal advection of heat by boundary currents is unlikely to explain the interannual variability of temperature around New Zealand, as it has in studies of the temperatures near the east coast of Australia (Hill et al. 2008; Wu et al. 2012; Oliver and Holbrook 2014). Temperature is highly correlated on both the western and eastern sides of the North Island of New Zealand (Fig. 3), wind stress curl over the South Pacific does not explain changes in East Auckland Current transport near Leigh (Stanton 2001), and currents off the west coast of the North Island are very weak in magnitude and fluctuate in direction (Sutton and Bowen 2011).

The heat flux between the atmosphere and the ocean clearly plays a role in the interannual variability of sea surface temperature in the region. Air–sea fluxes from the ECCOv4 upper-ocean heat balance are the largest contribution to the temperature anomaly in some years (Fig. 8). However, as Fig. 4 shows, estimates of heat fluxes vary considerably between the ocean reanalyses (ECCOv4 and GECCO), atmospheric reanalyses (JRA-55), and a product that includes more surface observations (OAFlux). Although the heat fluxes within ECCOv4 are consistent with the ocean observations and underlying model equations, there are clearly large uncertainties in determining the actual values of the flux.

We suggest that ocean heat transport convergence is playing a significant role in the upper-ocean heat balance (Fig. 8) and that it is related to large changes in the temperature at depth in the Tasman Sea along the XBT line. These results are consistent with previous studies: Sutton et al. (2005) note that deep and surface temperatures vary together along the PX34 XBT line, and Sprintall et al. (1995) suggest that a divergence of geostrophic flow in the Tasman Sea in the early 1990s "preconditions" the mixed layer for cooler temperatures. Surface temperatures are modified by deeper temperatures whenever water below the mixed layer is entrained into the mixed layer by vertical velocities or vertical mixing. While vertical velocities associated with Rossby and Kelvin waves vanish at the surface, the mixed layer extends tens of meters below the surface where vertical velocities are not zero. Vertical advection is likely to contribute to the signature of Rossby waves in

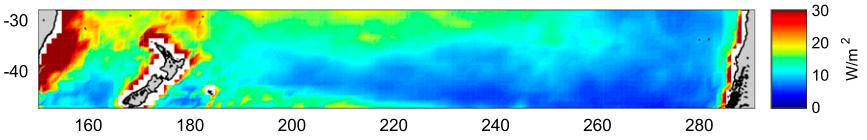

FIG. 10. The standard deviation of the vertical heat advection from the ECCOv4 ocean state estimate at a depth 50 m below the maximum mixed layer depth.

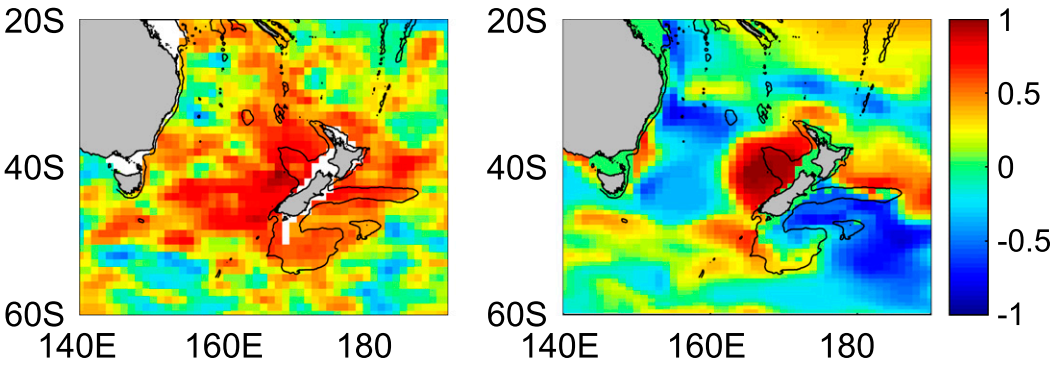

FIG. 11. The correlation of thermocline temperatures (temperatures averaged between 300 and 400 m) at a point south of Challenger Plateau with thermocline temperatures throughout the region in (left) the Argo product and (right) the ECCOv4 reanalysis.

ocean color observations by injecting nutrients into the mixed layer (Charria et al. 2006) and may also contribute to propagating features in sea surface temperatures observed in all the ocean basins (Hill et al. 2000).

We suggest that ocean heat transport convergence may be due to the adjustment of the thermocline around New Zealand from the arrival of wind-driven barotropic Rossby waves, as described in simulations by Hill et al. (2011). To investigate how widespread the movement of the thermocline is over the region, temperatures between 300 and 400 m from the Argo data near 41°S, 166°E, a location near the Tasman XBT line, are annually averaged and correlated with temperatures at the same depths around New Zealand (Fig. 11). Correlations of annually averaged temperatures at the same depths from ECCOv4 also show the thermocline in the Tasman Sea and off northeast New Zealand moves coherently (Fig. 11). Although from relatively short time series, the correlations are consistent with large-scale movement of the thermocline in the subtropical water around New Zealand. Sea level observations also show large-scale adjustment around the country consistent with the model simulations of Hill et al. (2011). Sea level at 36°S, 175°E, a location near Leigh, is highly correlated with sea level over a region largely coincident with the 1000-m isobath (Fig. 12), consistent with the propagation of coastal trapped waves around the country. Six months later the highest correlations are in the Tasman Sea to the west of the country. Westward propagation with phase speeds of a few cm s^{-1} are evident in sea level anomalies in the Tasman Sea and in the PX34 XBT temperatures, consistent with the radiation of baroclinic Rossby waves from the western side of New Zealand as seen in simulations (Hill et al. 2011) and expected from boundary wave theory (Marshall and Johnson 2013).

Our results show that the role of ocean heat transport convergence in the heat balance of the upper ocean deserves further investigation. If ocean heat transport convergence is responsible for some of the correlation of interannual temperatures and arrival of barotropic Rossby waves (Fig. 5), then this is a new mechanism for creating ENSO variability in subtropical sea surface

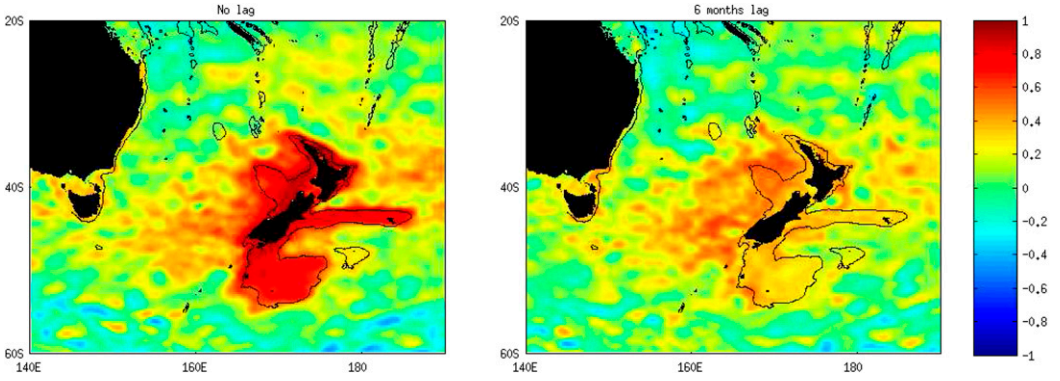

FIG. 12. The correlation of sea surface height near Leigh with sea level in the region at (left) zero lag and (right) 6-month lag.

temperatures, distinctly different from the ''imprinting'' of variability on the ocean by the atmosphere through air–sea heat flux that has been the focus of previous studies (e.g., Ciasto and England 2011; Fauchereau et al. 2003). Ocean heat transport convergence would also contribute to ENSO variability in the fluxes of sensible and latent heat between the ocean and the atmosphere. Quantifying the movement of heat between the upper ocean and deeper ocean will be critical to future understanding of interannual sea surface temperature variability.

Acknowledgments. We thank Estimating the Circulation and Climate of the Ocean (ECCO) Consortium for providing the ECCOv4 product, which can be downloaded from ftp://mit.ecco-group.org/ecco_for_las/version_4/release1/. The GECCO2 produced is from the Integrated Climate Data Center, University of Hamburg. The JRA-55 atmospheric reanalyses are available from http://rda.ucar.edu/datasets/ds628.0/. The OISST is available from http://www.esrl.noaa.gov/psd/data/gridded/data.noaa.oisst.v2.html. The Roemmich and Gilson climatology is available from http://sio-argo.ucsd.edu/RG_Climatology.html. Temperatures from the XBT lines in the Tasman Sea are available at http://www-hrx.ucsd.edu/index.html. The NZT7 anomalies are available from NIWA (https://www.niwa.co.nz/our-science/climate/information-and-resources/nz-temp-record/seven-station-series-temperature-data). Sea surface height and geostrophic velocities are available from AVISO (http://www.aviso.altimetry.fr/en/home.html). Leigh temperatures are available from the authors on request.

M.B. and P.S. were partially supported by the New Zealand Deep South National Science Challenge. J.M. would like to acknowledge support from the Friends of Leigh scholarship. X.Z. was supported by the Earth System and Climate Change Hub of the Australian Government's National Environmental Science Programme.

The authors thank three anonymous reviewers for constructive comments that greatly improved the manuscript.

REFERENCES

Bowen, M. M., P. J. H. Sutton, and D. Roemmich, 2006: Wind-driven and steric fluctuations of sea surface height in the southwest Pacific. *Geophys. Res. Lett.*, **33**, L14617, doi:10.1029/2006GL026160.

Charria, G., I. Dadou, P. Cipollini, M. Drévillon, P. De Mey, and V. Garçon, 2006: Understanding the influence of Rossby waves on surface chlorophyll concentrations in the North Atlantic Ocean. *J. Mar. Res.*, **64**, 43–71, doi:10.1357/002224006776412340.

Ciasto, L. M., and D. W. J. Thompson, 2009: Observational evidence of reemergence in the extratropical Southern Hemisphere. *J. Climate*, **22**, 1446–1453, doi:10.1175/2008JCLI2545.1.

——, and M. H. England, 2011: Observed ENSO teleconnections to Southern Ocean SST anomalies diagnosed from a surface mixed layer heat budget. *Geophys. Res. Lett.*, **38**, L09701, doi:10.1029/2011GL046895.

de Boyer Montgut, C., G. Madec, A. S. Fischer, A. Lazar, and D. Iudicone, 2004: Mixed layer depth over the global ocean: An examination of profile data and a profile-based climatology. *J. Geophys. Res.*, **109**, C12003, doi:10.1029/2004JC002378.

Deser, C., M. A. Alexander, and M. S. Timlin, 2003: Understanding the persistence of sea surface temperature anomalies in midlatitudes. *J. Climate*, **16**, 57–72, doi:10.1175/1520-0442(2003)016<0057:UTPOSS>2.0.CO;2.

——, ——, S.-P. Xie, and A. S. Phillips, 2010: Sea surface temperature variability: Patterns and mechanisms. *Annu. Rev. Mar. Sci.*, **2**, 115–143, doi:10.1146/annurev-marine-120408-151453.

Ducet, N., and P. Y. LeTraon, 2000: Global high-resolution mapping of ocean circulation from TOPEX/Poseidon and ERS-1 and -2. *J. Geophys. Res.*, **105**, 19 477–19 498, doi:10.1029/2000JC900063.

Emery, W. J., and R. E. Thomson, 2001: Data Analysis Methods in Physical Oceanography. Elsevier, 654 pp.

Evans, J., and J. Atkins, 2008: Seawater temperature dataset at Goat Island, Leigh, New Zealand from 1967 to 2011. University of Auckland. [Available online at https://hdl.handle.net/2292/20612.]

Fauchereau, N., S. Trzaska, Y. Richard, P. Roucou, and P. Camberlin, 2003: Sea-surface temperature co-variability in the southern Atlantic and Indian Oceans and its connections with the atmospheric circulation in the Southern Hemisphere. *Int. J. Climatol.*, **23**, 663–677, doi:10.1002/joc.905.

Folland, C., and M. Salinger, 1995: Surface temperature trends and variations in New Zealand and the surrounding ocean, 1871–1993. *Int. J. Climatol.*, **15**, 1195–1218, doi:10.1002/joc.3370151103.

Forget, G., J.-M. Campin, P. Heimbach, C. N. Hill, R. M. Ponte, and C. Wunsch, 2015: ECCO version 4: An integrated framework for non-linear inverse modeling and global ocean state estimation. *Geosci. Model Dev.*, **8**, 3071–3104, doi:10.5194/gmd-8-3071-2015.

Frankignoul, C., P. Müller, and E. Zorita, 1997: A simple model of the decadal response of the ocean to stochastic wind forcing. *J. Phys. Oceanogr.*, **27**, 1533–1546, doi:10.1175/1520-0485(1997)027<1533:ASMOTD>2.0.CO;2.

Godfrey, J. S., 1989: A Sverdrup model of the depth-integrated flow for the world ocean allowing for island circulations. *Geophys. Astrophys. Fluid Dyn.*, **45**, 89–112, doi:10.1080/03091928908208894.

Greig, M., N. M. Ridgway, and B. S. Shakespeare, 1988: Sea surface temperature variations at coastal sites around New Zealand. *N. Z. J. Mar. Freshwater Res.*, **22**, 391–400, doi:10.1080/00288330.1988.9516310.

Guan, Y., B. Huang, J. Zhu, Z.-Z. Hu, and J. L. Kinter, 2014: Interannual variability of the South Pacific Ocean in observations and simulated by the NCEP Climate Forecast System, version 2. *Climate Dyn.*, **43**, 1141–1157, doi:10.1007/s00382-014-2148-y.

Hill, K. L., I. S. Robinson, and P. Cipollini, 2000: Propagation characteristics of extratropical planetary waves observed in the ATSR global sea surface temperature record. *J. Geophys. Res.*, **105**, 21 927–21 945, doi:10.1029/2000JC900067.

——, S. R. Rintoul, R. Coleman, and K. R. Ridgway, 2008: Wind forced low frequency variability of the East Australian Current. *Geophys. Res. Lett.*, **35**, L08602, doi:10.1029/2007GL032912.

——, ——, K. Ridgway, and P. R. Oke, 2011: Decadal changes in the South Pacific western boundary current system revealed in observations and ocean state estimates. *J. Geophys. Res.*, **116**, C01009, doi:10.1029/2009JC005926.

Holbrook, N. J., and N. L. Bindoff, 1997: Interannual and decadal temperature variability in the southwest Pacific Ocean between 1955 and 1988. *J. Climate*, **10**, 1035–1049, doi:10.1175/1520-0442(1997)010<1035:IADTVI>2.0.CO;2.

Kobayashi, S., and Coauthors, 2015: The JRA-55 Reanalysis: General specification and basic characteristics. *J. Meteor. Soc. Japan*, **93**, 5–48, doi:10.2151/jmsj.2015-001.

Köhl, A., 2015: Evaluation of the GECCO2 ocean synthesis: Transports of volume, heat and freshwater in the Atlantic. *Quart. J. Roy. Meteor. Soc.*, **141**, 166–181, doi:10.1002/qj.2347.

Marshall, D. P., and H. L. Johnson, 2013: Propagation of meridional circulation anomalies along western and eastern boundaries. *J. Phys. Oceanogr.*, **43**, 2699–2717, doi:10.1175/JPO-D-13-0134.1.

Mullan, A. B., S. J. Stuart, M. G. Hadfield, and M. J. Smith, 2010: Report on the review of NIWA's 'Seven-Station' temperature series. Tech. Rep. NIWA Information Series 78, 175 pp.

Oliver, E. C. J., and N. J. Holbrook, 2014: Extending our understanding of South Pacific gyre "spin-up": Modeling the East Australian Current in a future climate. *J. Geophys. Res. Oceans*, **119**, 2788–2805, doi:10.1002/2013JC009591.

Reynolds, R. W., N. A. Rayner, T. M. Smith, D. C. Stokes, and W. Wang, 2002: An improved in situ and satellite SST analysis for climate. *J. Climate*, **15**, 1609–1625, doi:10.1175/1520-0442(2002)015<1609:AIISAS>2.0.CO;2.

Rintoul, S. R., and M. H. England, 2002: Ekman transport dominates local air–sea fluxes in driving variability of subantarctic mode water. *J. Phys. Oceanogr.*, **32**, 1308–1321, doi:10.1175/1520-0485(2002)032<1308:ETDLAS>2.0.CO;2.

Roberts, C. D., M. D. Palmer, R. P. Allan, D. G. Desbruyeres, P. Hyder, C. Liu, and D. Smith, 2017: Surface flux and ocean heat transport convergence contributions to seasonal and interannual variations of ocean heat content. *J. Geophys. Res.*, **122**, 726–744, doi:10.1002/2016JC012278.

Roemmich, D., and J. Gilson, 2009: The 2004–2008 mean and annual cycle of temperature, salinity, and steric height in the global ocean from the Argo Program. *Prog. Oceanogr.*, **82**, 81–100, doi:10.1016/j.pocean.2009.03.004.

Sasaki, Y. N., S. Minobe, N. Schneider, T. Kagimoto, M. Nonaka, and H. Sasaki, 2008: Decadal sea level variability in the South Pacific in a global eddy-resolving ocean model hindcast. *J. Phys. Oceanogr.*, **38**, 1731–1747, doi:10.1175/2007JPO3915.1.

Sharples, J., 1997: Cross-shelf intrusion of subtropical water into the coastal zone of northeast New Zealand. *Cont. Shelf Res.*, **17**, 835–857, doi:10.1016/S0278-4343(96)00060-X.

Sprintall, J., D. Roemmich, B. Stanton, and R. Bailey, 1995: Regional climate variability and ocean heat transport in the southwest Pacific Ocean. *J. Geophys. Res.*, **100**, 15 865–15 871, doi:10.1029/95JC01664.

Stanton, B. R., 2001: Estimating the East Auckland Current transport from model winds and the Island Rule. *N. Z. J. Mar. Freshwater Res.*, **35**, 531–540, doi:10.1080/00288330.2001.9517020.

Sutton, P. J. H., and M. M. Bowen, 2011: Currents off the west coast of Northland, New Zealand. *N. Z. J. Mar. Freshwater Res.*, **45**, 609–624, doi:10.1080/00288330.2011.569729.

——, ——, and D. Roemmich, 2005: Decadal temperature changes in the Tasman Sea. *N. Z. J. Mar. Freshwater Res.*, **39**, 1321–1329, doi:10.1080/00288330.2005.9517396.

Ummenhofer, C., and M. H. England, 2007: Interannual extremes in New Zealand precipitation linked to modes of Southern Hemisphere climate variability. *J. Climate*, **20**, 5418–5440, doi:10.1175/2007JCLI1430.1.

Verdy, A., J. Marshall, and A. Czaja, 2006: Sea surface temperature variability along the path of the Antarctic Circumpolar Current. *J. Phys. Oceanogr.*, **36**, 1317–1331, doi:10.1175/JPO2913.1.

Wu, L., and Coauthors, 2012: Enhanced warming over the global subtropical western boundary currents. *Nat. Climate Change*, 2, 161–166, doi:10.1038/nclimate1353.

Yu, L., and R. A. Weller, 2007: Objectively analyzed air–sea heat fluxes for the global ice-free oceans (1981–2005). *Bull. Amer. Meteor. Soc.*, **88**, 527–539, doi:10.1175/BAMS-88-4-527.

Zeldis, J. R., R. A. Walters, M. J. N. Greig, and K. Image, 2004: Circulation over the northeastern New Zealand continental slope, shelf and adjacent Hauraki Gulf, during spring and summer. *Cont. Shelf Res.*, **24**, 543–561, doi:10.1016/j.csr.2003.11.007.